



HAL
open science

A mask-based diagnostic platform for point-of-care screening of Covid-19

John Daniels, Shekhar Wadekar, Ken Decubellis, George Jackson, Alexander Chiu, Quentin Pagneux, Hiba Saada, Ilka Engelmann, Judith Ogiez, Delphine Loze-Warot, et al.

► To cite this version:

John Daniels, Shekhar Wadekar, Ken Decubellis, George Jackson, Alexander Chiu, et al.. A mask-based diagnostic platform for point-of-care screening of Covid-19. *Biosensors and Bioelectronics*, 2021, 192, pp.113486. 10.1016/j.bios.2021.113486 . hal-03442228

HAL Id: hal-03442228

<https://hal.science/hal-03442228v1>

Submitted on 2 Aug 2023

HAL is a multi-disciplinary open access archive for the deposit and dissemination of scientific research documents, whether they are published or not. The documents may come from teaching and research institutions in France or abroad, or from public or private research centers.

L'archive ouverte pluridisciplinaire **HAL**, est destinée au dépôt et à la diffusion de documents scientifiques de niveau recherche, publiés ou non, émanant des établissements d'enseignement et de recherche français ou étrangers, des laboratoires publics ou privés.



Distributed under a Creative Commons Attribution - NonCommercial 4.0 International License

A Mask-Based Diagnostic Platform for Point-of-Care Screening of Covid-

19

John Daniels,^{1*} Shekhar Wadekar,¹ Ken DeCubellis,¹ George W. Jackson,² Alexander S. Chiu,² Quentin Pagneux,³ Hiba Saada,³ Ilka Engelmann,⁴ Judith Ogiez,⁴ Delphine Loze-Warot,⁵

Rabah Boukherroub^{3*} and Sabine Szunerits^{3*}

¹ *Diagmetrics Inc., 30 Renees Way Madison, Connecticut, USA 06443.*

² *Base Pair Biotechnologies, Inc., 8619 Broadway St., Suite 100, Pearland, TX, USA*

³ *Univ. Lille, CNRS, Centrale Lille, Univ. Polytechnique Hauts-de-France, UMR 8520 - IEMN, F-59000 Lille, France*

Univ Lille, CHU Lille, Laboratoire de Virologie ULR3610, F-59000 Lille, France

⁵ *CerbaHealthCare Biomedical Laboratory, CERBALLIANCE Lille, 17/24 rue de la Digue 59000 Lille.*

Abstract

Diagnostics of SARS-CoV-2 infection using real-time reverse-transcription polymerase chain reaction (RT-PCR) on nasopharyngeal swabs is now well-established, with saliva-based testing being lately more widely implemented for being more adapted for self-testing approaches. In this study, we introduce a different concept based on exhaled breath condensates (EBC), readily collected by a mask-based sampling device, and detection with an electrochemical biosensor with a modular architecture that enables fast and specific detection and quantification of COVID-19. The face mask forms an exhaled breath vapor containment volume to hold the exhaled breath vapor in proximity to the EBC collector to enable a condensate-forming surface, cooled by a thermal mass, to coalesce the exhaled breath into 200-500 μL fluid sample in 2 minutes. EBC RT-PCR for SARS-CoV-2 genes (E, ORF1ab) on samples collected from 7 SARS-CoV-2 positive and 7 SARS-CoV-2 negative patients were performed. The presence of SARS-CoV-2 could be detected in 5 out of 7 SARS-CoV-2 positive patients. Furthermore, the EBS samples were screened on an electrochemical aptamer biosensor, which detects SARS-CoV-2 viral particles down to 10 pfu mL^{-1} in cultured SARS-CoV-2 suspensions. Using a “turn off” assay via ferrocenemethanol of redox mediator, results about the infectivity state of the patient are obtained in 10 min.

Keywords: Exhaled breath condensate (EBC); aptamers, SARS-CoV-2; detection; electrochemistry; real-time reverse-transcription polymerase chain reaction (RT-PCR)

1. Introduction

While other human coronaviruses, e.g. HCoV-229E and HCoV-OC43, have only induced mild common cold effects, the SARS-CoV-2 pandemic has caused more than 2.77 M death worldwide (as for 27 March 2021) with 126 M cases detected. Infection with SARS-CoV-2 is diagnosed worldwide using nasopharyngeal swab samples and more recently saliva samples by detection of SARS-CoV-2 RNA using real-time reverse-transcription polymerase chain reaction (RT-PCR). The procedure to obtain nasal swab samples is not only uncomfortable, but requires specialized personal with risk of contaminating the person performing the test. Saliva tests have the advantage of being simpler to perform, less invasive with limited risks and RT-PCR on saliva specimens has becoming more widely implemented (Ryan *et al.*, 2021, Ter-Ovanesyan *et al.*, 2021, Wyllie *et al.*, 2020). The viscose nature of saliva together with the presence of saliva proteases, responsible for the proteolytic activity of saliva, make the direct application of saliva samples challenging. It is well known that the major mechanisms of COVID-19 spread are airborne and contact infections primarily due to the high resistance of the virus once in aerosol droplets expelled from infected persons. Given the growing need for sample collection by patients themselves, exhaled breath condensate (EBC) (Khoubnasabjafari *et al.*, 2020, Ryan *et al.*, 2021) might represent an important alternative specimen type for SARS-CoV-2 diagnostic.

Different than exhaled breath (EB), which is based on exhalation of volatile organic compounds (VOCs NO, CO₂, NH₃, H₂O₂, etc.) (Shan *et al.*, 2020), EBC contains lower respiratory droplets which can be analyzed by RT-PCR (Ryan *et al.*, 2021). Indeed, EBC RT-PCR has been already investigated to identify other respiratory viruses, including human coronaviruses with the aim to gain knowledge about the efficiency of face mask (Leung *et al.*, 2020). Ryan and coworkers reported preliminary data from patients with a positive and negative RT-PCR tests for SARS-CoV-2 where EBC was collected in addition using commercial RTube condensers. RT-PCR of EBC collected samples was positive for SARS-CoV-2 for 21 out of 31 cases (68%) using the E and S proteins assay specific kits and increased to 93.5% using four targets (S, E, NP, ORF1ab) (Ryan *et al.*, 2021). This study strongly supports the hypothesis that EBC collected samples are suitable for SARS-CoV-2 detection. These findings and the possibility to collect EBC from patients during tidal breathing and coughing into a mask prompted us to investigate this non-invasive sample collection method in combination with an electrochemical point-of-care testing (POCT) system for the discrimination between infected SARS-CoV-2 and healthy patients (**Figure 1**).

In this work, we take the opposite approach of that investigated by Cowling et al (Leung et al., 2020) and propose a face mask to collect EBC. To date only specific devices have been proposed to collect and condensate exhaled breath.

We show, in this work, the utility of an aptamer-based electrochemical biosensor. Aptamers exhibit many advantages as recognition elements when compared to traditional antibodies due their small size, enhanced chemical stability and low cost of production (Yoo et al., 2020). We report notably on an electrochemical sensing format targeting the spike protein (S) which is embedded in a lipidic membrane forming the SARS-CoV-2 viral outer wall. The spike protein protrudes from the viral membrane, and the viral entry into host cells is mediated by the receptor-binding domain (RBD) region of the spike protein that recognizes the host receptor ACE2. With the spike protein being repeated about 50-200 times on the viral surface (Wrapp et al., 2020), the RBD region of the S protein represents therefore an excellent diagnostic target. The aptamer chosen in this work is a 32-nucleotide aptamer from Base Pair Biotechnologies (Pearland, Texas, USA).

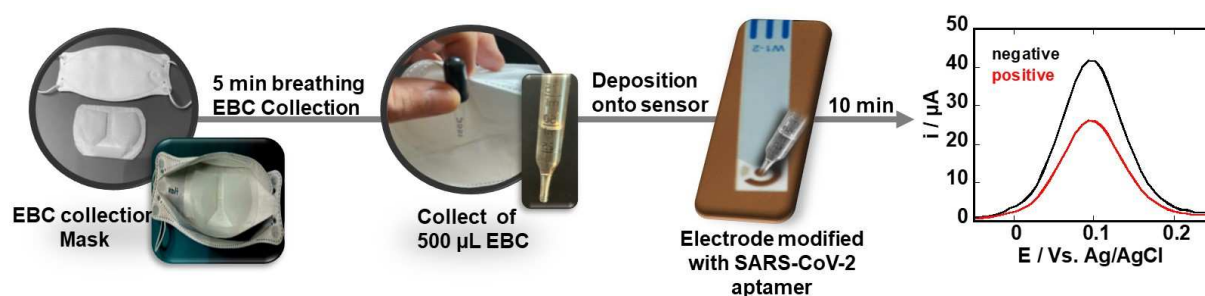


Figure 1: Exhaled breath condensate (EBC) based diagnostic strategy for SARS-CoV-2 infectivity: Laboratory engineered mask allows collection of EBC by first cooling the mask for 30 min in the freezer, putting on the cooled mask and breathing into it for 5 min. EBS formed in the Teflon-lining of the inside of the masks is collected and directly deposited onto an electrochemical sensing modified with SARS-CoV-2 specific aptamer targeting the receptor-binding domain (RBD) region of the S1 spike protein as surface receptor. Using ferrocenemethanol as redox mediator before and after viral interaction allows discrimination between positive and negative EBC samples.

2. Results and Discussion

2.1. Collection of Exhaled Breath Condensate

The mask-based EBC collection system is based on commercial face mask fitted with an engineered EBC collector system based on a Teflon coated cooling trap (**Figure 2a**). To increase the EBC collection efficiency, the mask is placed into a freezer -20°C for 30 min, before being placed over the mouth of the person to be tested. This polytetrafluoroethylene (PTFE) trap when cooled allows sample liquification on its surface, where the formed droplets can be collected with a pipette and used for analysis directly. The presence of a collection pool at the end of this cooling pool allows further collection of EBC (**Figure 2b**) without the need for technical expertise (**Figure S1**). During the EBC collection the inside of the mask is not exposed to air and the risk of contamination of the EBC samples is negligible. Using this collection system, $400\pm 150\ \mu\text{L}$ of EBC can be collected within 5 min (**Figure 2c**).

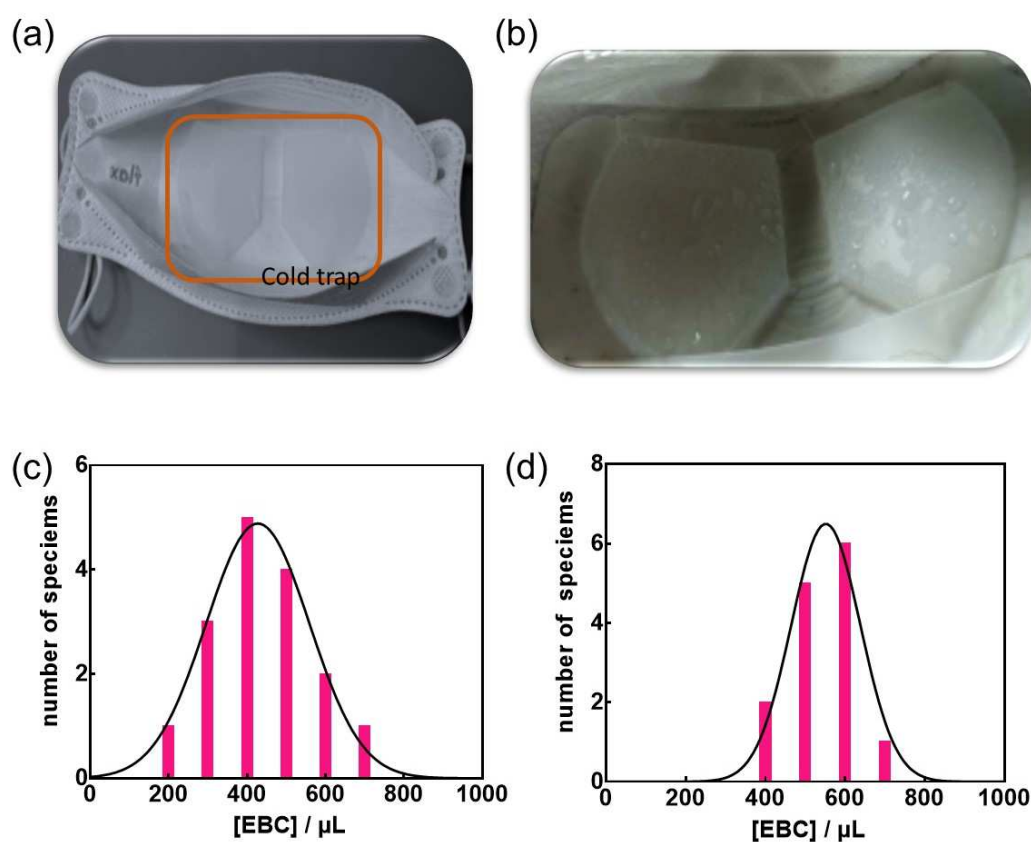


Figure 2: Mask-based EBC collector: (a) Inside of the laboratory engineered mask showing an exhaled breath condensate (EBC) collector (cold trap, indicated with orange line) for converting breath vapor into a fluid sampling. The EBC collector is made of a Teflon-based condensate-forming surface. (b) Image of EBC formed on the Teflon collector after 5 min breathing into the mask. (c) EBC volume collected in 5 min using the EBC Mask (n=14). (d) EBC volume collected in 5 min using commercial RTube condensers (n=14).

The collection efficiency was comparable to EBC collected by commercial RTube condensers (Respiratory Research Inc., USA) (**Figure 2d**). The collection efficiency is person-dependent as seen in **Figure 2c**. However, in most cases the required 300 μL needed for further analysis was obtained in this manner. While indeed, collection of an equal volume of saliva is more efficient at a 5 min time span, saliva is a complex sample matrix containing proteases and other variable components that can impact most assays. This includes the potential degradation of the SARS-CoV-2 S1 protein targeted by the aptamer employed in this test. The much cleaner EBC sample is therefore believed to be more suitable and reliable for rapid testing.

2.2. SARS-CoV-2 aptamer and electrochemical sensor

The SARS-CoV-2 aptamer targeting the S1 protein was selected *via* combinatorial libraries of nucleic acid sequences by the SELEX (systemic evolution of ligands by exponential enrichment) process. As seen in **Figure 3a**, the aptamer investigated in this work is a 20-base aptamer “CFA0688T” (Base Pair Bio) with 1 loop modified on the 5' end with a thiol-TTT-TTT to give the aptamer some flexibility for its anchoring onto gold interfaces. The binding affinity to the recombinant SARS-CoV-2 S1 spike protein was determined by Biolayer interferometry (BLI) measurements and was determined as $K_D=3.52\pm 0.17$ nM ($R^2 = 0.9985$) (**Figure 3b**). This affinity value is comparable to other reported SARS-CoV-2 aptamers such as the 51-base pair aptamer with 3 hair-pined structures selective to RBD reported by Song *et al.* (Song *et al.*, 2020) or the 58-base pair aptamer proposed by Torabi *et al.* (Torabi *et al.*, 2020) with K_D values ranging from 5.8 ± 0.8 nM (Song *et al.*, 2020) to 0.49 ± 0.05 nM (Torabi *et al.*, 2020).

The attachment of the SARS-CoV-2 aptamer to screen printed electrodes (SPE) was achieved via a maleimide functionalized poly(ethylene glycol) (PEG) spacer, a commonly employed hydrophilic polymer to avoid biofouling and used for cysteine-modified aptamer integration by others (Da Pieve *et al.*, 2010). The spacer aids in overcoming any potential steric hindrance in viral detection. The success of the linking strategy was validated using XPS (See SI, **Figure S2**).

A key concept in electrochemical systems is the fact that the kinetics of the heterogeneous electron transfer at modified electrodes is strongly dependent on the surface coverage and on the thickness of the modifying layer (Cannes *et al.*, 2003). **Figure 3d** depicts the cyclic

voltammograms of the gold working electrode before and after modification with the aptamer using ferrocenemethanol as a redox mediator. This small mediator can permeate to a small extent into a monolayer modified gold electrode or *via* diffusion through pinholes with electron transfer occurring at the free sites on the electrode. As expected, a decrease in electron transfer is observed in line with the presence of the aptamer on the electrode surface.

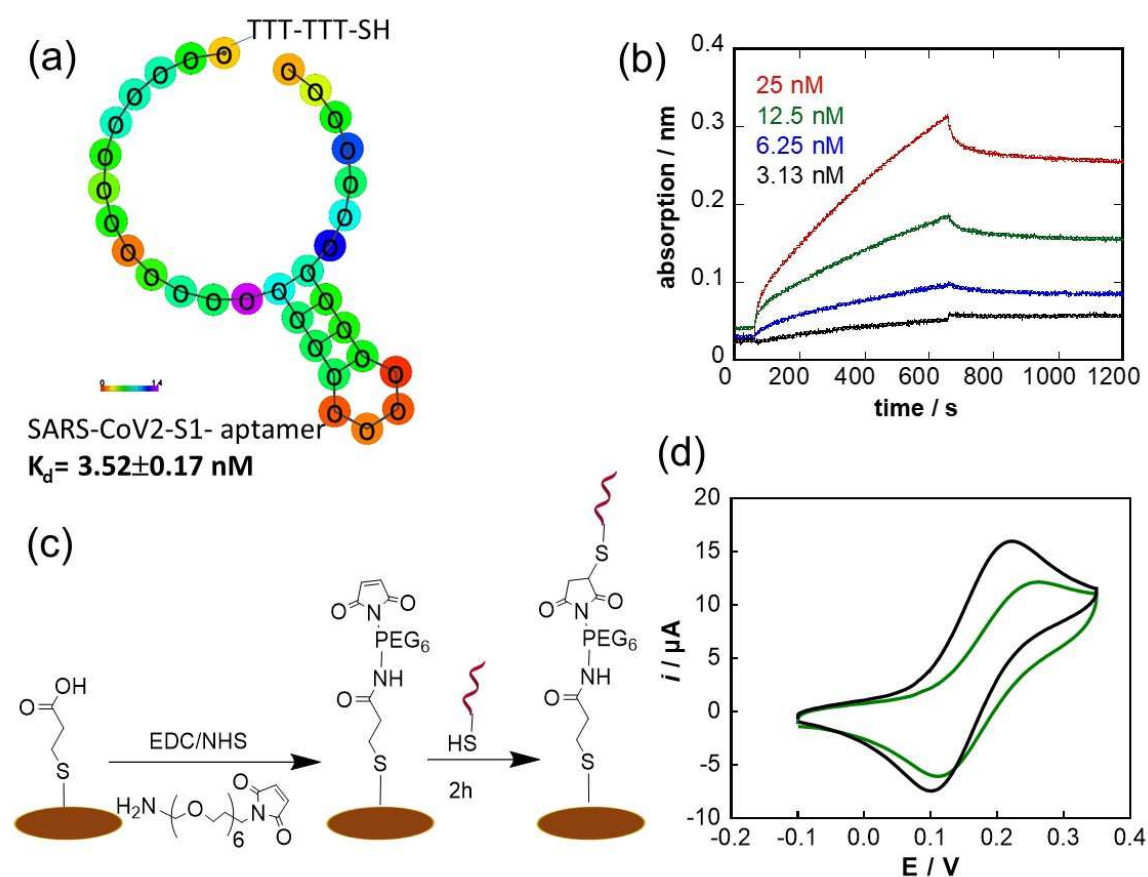


Figure 3: Electrochemical Aptamer Sensor: (a) 2D structure of DNA aptamer with sequence redacted, (b) Bi-layer interferometry (BLI) measurements of biotinylated aptamer linked onto streptavidin-activated BLI sensors with different concentrations of SARS-CoV-2 S protein (3.13 nM, 6.25 nM, 12.5 nM and 25 nM): running buffer: 1x PBS, 1 mM MgCl₂, (c) Surface attachment strategy of SARS-Cov-2 aptamer on the gold working electrode of the screen-printed electrode using maleimide-thiol-aptamer linkage. (d) Cyclic voltammograms (CV) of a gold electrode before (black) and after (green) functionalization with SARS-CoV-2 aptamer (10 µg mL⁻¹ for 2 h) using ferrocenemethanol as a redox mediator (1 mM in 0.1 M PBS, pH 7.4, Scan rate=100 mV s⁻¹).

Analysis of 50 nM receptor domain binding from solution to the aptamer modified electrodes shows a clear decrease in current (**Figure 4a**). This decrease in current is linear up to [RBD]=10 nM, reaching complete saturation at 50 nM (**Figure 4b**). The corresponding curve can be fitted with the Langmuir isotherm (**Figure 4c**) using the following equation:

$$\Theta = j(c_0) / j(c_\infty) = K_A \times c_0 / (1 + K_A \times c_0)$$

With Θ being the surface coverage, $j(c_0)$ the current density at a given RBD concentration, $j(c_\infty)$ the current density at infinite bulk analyte concentration; assuming a 1:1 complex between the antigen (RBD) from solution and the aptamer receptor allows estimating the affinity constant K_A . From the expected S-shaped curve, a dissociation constant (i.e. a half saturation-constant) $K_D = 1.6 \pm 0.9$ nM could be determined indicating high affinity of the aptamer for RBD, and in line with reported nanomolar dissociation constants for aptamer-protein interactions (Manochehry et al., 2019, Vinkenberg et al., 2012) as well as independent affinity measurements made by Base Pair using biolayer interferometry (**Figure 3b**).

These interfaces were investigated for their potential to sense cultured SARS-CoV-2 viral particles (**Figure 4d**). Immersion of the sensor into PBS (0.1 M, pH 7.4) containing different concentrations of a SARS-CoV-2 isolate shows that the limit of detection (LOD), defined as the lowest level that an analyte can be reliably distinguished from the background, correlates to about 10 pfu mL⁻¹ (correlating to a current difference of 2 μ A) with a saturation at 1.5×10^5 pfu mL⁻¹. The detection limit was determined to be about 3 pfu mL⁻¹ from five blank noise signals (95% confidential level). The analytical performance was compared to that of SPE where the thiol-terminated aptamer was directly linked onto the gold surface (**Figure S3**). From the analysis of RBD binding to the aptamer a higher dissociation constant of $K_D = 6.2 \pm 1.2$ nM was determined. More importantly sensing of cultured SARS-CoV-2 viral particles indicates a LOD of about 200 pfu mL⁻¹.

This sensing sensitivity of the maleimide-thiol aptamer sensor is comparable to other electrochemical (Saroglia et al., 2021, Szunerits et al., 2021, Zhang et al., 2020) and electrical (Seo et al., 2020) sensors reported thus far in the literature. In addition, the possibility of detecting the variants 20I/501Y.V1 (called “British variant”) and 20H/501Y.V2 (called “South African variant”) was investigated by using SARS-CoV-2 variant isolates. **Figure 4c** indicates that the aptamer-based sensor senses variant the 20I/501Y.V1e and the 20H/501Y.V2 variant equally well. This is in line with results using commercial recombinant SARS-CoV-2 S protein considering the different mutations (SI, **Figure S4**). Indeed using

BLI measurements the affinity of the SARS-CoV-2 S protein UK variant to the aptamer is $K_D = 6.0 \pm 3 \text{ nM}$ with a $k_{on} = (1.52 \pm 0.003) \times 10^5 \text{ M}^{-1}\text{s}^{-1}$ while in the cases of the South African variant is $K_D = 1.6.0 \pm 0.1 \text{ nM}$ with a $k_{on} = (1.62 \pm 0.05) \times 10^5 \text{ M}^{-1}\text{s}^{-1}$. This is in the same order as the affinity constant of $3.52 \pm 0.17 \text{ nM}$ for the wild type (Wuhan) variant (**Figure 3b**)

The reproducibility of the SARS-CoV-2 aptamer electrodes was expressed in terms of the relative standard deviation, which was determined to be 2.3 % at a viral concentration of 10^3 pfu mL^{-1} ($n=5$). The long-term stability of the sensor when stored in PBS was also evaluated showing a loss of 2.5 % in the anodic peak current when testing virus solutions of 10^3 pfu mL^{-1} solution after the electrode has been stored at $4 \text{ }^\circ\text{C}$ for 1 month. To illustrate the selectivity of the sensor, the aptamer sensor was incubated with other viral samples, obtained by nasal swaps.

Testing on other coronaviruses producing symptoms close to those associated to SARS-CoV-2, HCoVOC43 and HCoV NL63, showed decreased interaction with the aptamer-interface as identified with a current difference smaller compared to the current difference recorded on a positive nasopharyngeal swab sample (**Figure 4e**). The same was observed for Influenza A (H1N1) and influenza B samples.

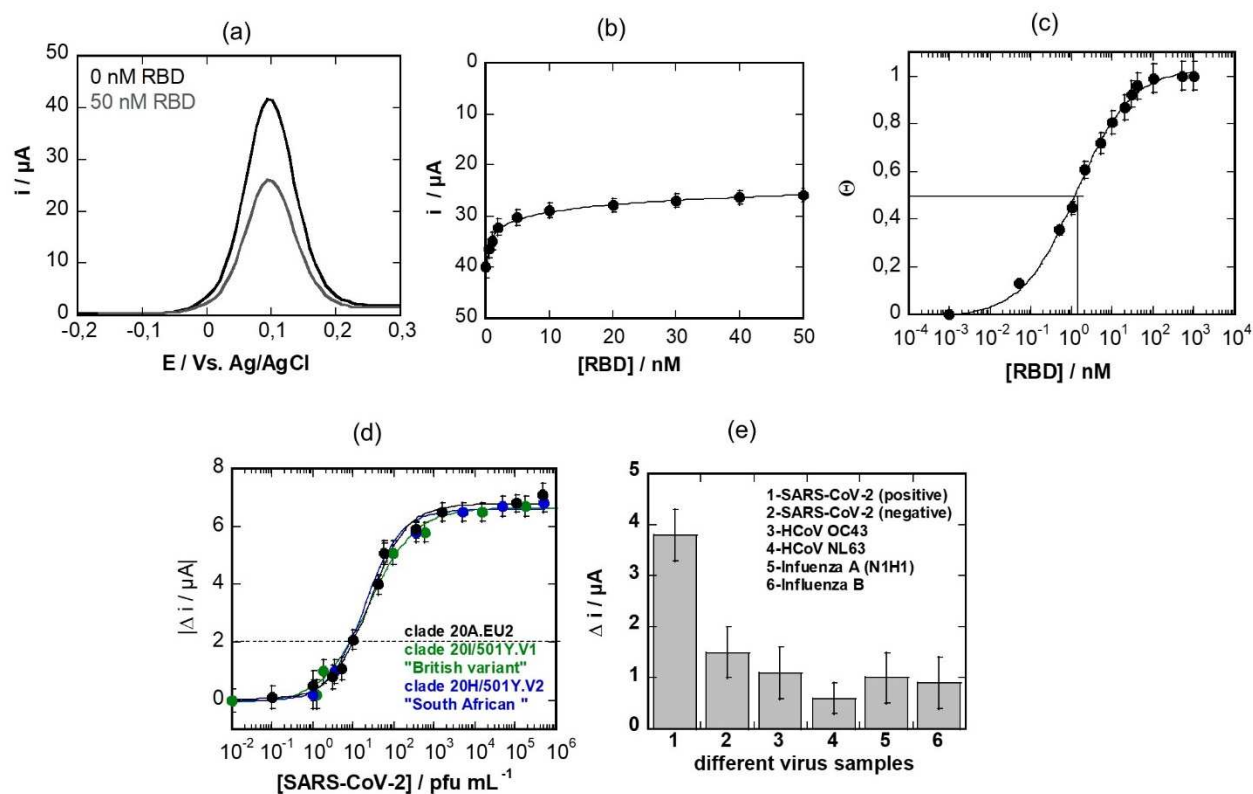


Figure 4: Electrochemical SARS-CoV-2 aptasensor: (a) Differential pulse voltammogram (DPV) of aptamer modified electrode using ferrocenemethanol (1 mM in 0.1 M PBS, pH 7.4)

as redox mediator. Initial signal (black) and after addition 50 nM RBD for 10 min (grey line), washing and recording a new DPV in ferrocenemethanol. The decrease in current is due to RBD binding to the aptamer. DPV conditions: $t_{\text{acq}}=3\text{s}$, $E_{\text{step}}=0.01\text{V}$, $E_{\text{pulse}}=0.06\text{V}$, $t_{\text{pulse}}=0.02\text{V}$, scan rate= 0.06V s^{-1} . (b) Current response to increasing RBD concentrations using ferrocenemethanol (1 mM PBS, pH 7.4) as a redox probe. (c) Langmuir adsorption isotherm as extracted from Figure 4b. (d) Dose-dependent response curve toward SARS-CoV-2 virus clade 20A.EU2 (black) as well as clade 20I/501Y.V1, “British variant” (green) and the clade 20H/501Y.V2, “South African variant” (blue) on aptamer modified electrodes. (e) Selectivity of the aptamer sensors diagnostics towards other real patient virus samples by comparison to SARS-CoV-2 positive samples. All the virus samples have Ct values between 22-25 respectively and are nasal swab samples. All the values are displayed as means \pm SEM (n=5).

2.3. Exhaled breath condensate analysis

Given that the disease is transmitted via exhaled droplets, and that EBC is the established modality for sampling exhaled aerosol, detection of SARS-CoV-2 in EBC is a promising approach for safe and efficient diagnosis of the disease (Khoubnasabjafari et al., 2020). We validated the possibility of SARS-CoV-2 sensing using EBC collected by commercial Rtube condensers and EBC mask-based system. EBC samples were collected using a cold trap as shown in **Figure 1**. In parallel, nasopharyngeal swab samples also were collected.

In a proof of principle study, EBC samples of 14 volunteers were collected and analyzed by PCR (**Table 1**). Out of the 14 nasopharyngeal swab samples, seven were identified as SARS-CoV-2 positive and seven as SARS-CoV-2 negative (Cycle threshold (C_t) >40) by targeting the N structural protein as well as the RNA dependent RNA polymerase (RdRp) nonstructural protein via RT-PCR. Based on our experiments with different dilutions of a SARS-CoV-2 isolate, we estimated that a C_t of 34 approximately corresponds to about 10^4 copies of viral RNA per milliliter and that this dilution showed no infectivity to Vero cells. The lower C_t values of 22 (**Table 1**) correlated to about 10^7 copies of viral RNA per milliliter.

The results of EBC RT-PCR performed on samples collected by Rtube condensers as well as EBC masks of the SARS-CoV-2 negative patients were in full agreement with that of nasopharyngeal swab samples (7/7, 100%). Testing these samples on the electrochemical sensor, where a current difference higher than $2\ \mu\text{A}$ (**Figure 4d**) was considered to be linked to the presence of viral particles, resulted in further identification of these sample as SARS-CoV-2 negative.

In the case of EBC samples collected from patients identified by nasopharyngeal RT-PCR as SARS-CoV-2 positive, 3 samples out of 7 were identified as SARS-CoV-2 positive using the commercial RTube condenser and 5/7 using the face mask using a Ct of 40 as cut-off. In contrast to the nasopharyngeal samples, the Ct values of the RdRp gene detected in the EBS samples were always considerably lower than the N-gene (**Table 1**). The difference in the Ct values between nasal swab samples and EBC is linked to the different viral load present in both fluids. (Eiche et al., 2020, Giovannini et al., 2021). Indeed, it has been postulated that the viral load of SARS-CoV-2 in aerosol samples is several orders of magnitude below those in nasopharyngeal swabs, which are in the order of 6.41×10^2 - 1.34×10^{11} copies/mL (Giovannini et al., 2021). This indicates that the N-gene is likely the more robust gene to target for EBC samples independently on the collection strategy applied. Testing the mask-collected EBC collected samples on the aptamer electrochemical sensor showed agreement with EBC RT-PCR results using masks. This indicates that such sensors are well-adapted for sensing EBC viral samples and further confirms the presence of active viral particles in exhaled breath of SARS-CoV-2 positive patients

Table 1: Exhaled breath condensate studies on patients identified by nasopharyngeal swabs RT-PCR as SARS-CoV-2 positive (black numbers) or negative (red numbers).

Volunteer	Ct ¹ values (N gene/RdRp1) ² of nasal swabs	Ct values (N gene/RdRp1) ¹ of EBC collected with Rtube	Ct values (N gene/RdRp1) ¹ of EBC collected with mask	$\Delta i / \mu A$ of aptamer-sensor ² on EBC of masks
Patients identified as SARS-CoV-2 Positive				
1	22.6 / 28.7	>40 / >40	>40 / >40	1.4 (Negative)
2	26.9 / 26.1	>40 / >40	32.9 / 37.5	2.6 (Positive)
3	33.1 / 25.8	32.2 / 38.7	33.3 / 38.6	2.3 (Positive)
4	25.4 / 21.1	31.7 / 37.5	32.2 / 37.5	2.2 (Positive)
5	26.8 / 19.6	32.7 / 38.9	33.7 / 36.5	2.3 (Positive)
6	26.5 / 21.1	>40 / >40	32.7 / 37.3	2.4 (Positive)
7	33.2 / 25.9	>40 / >40	>40 / >40	1.2 (Negative)
Patients identified as SARS-CoV-2 Negative				
8	>40 / >40	>40 / >40	>40 / >40	0.5 (Negative)
9	>40 / >40	>40 / >40	>40 / >40	1.5 (Negative)
10	>40 / >40	>40 / >40	>40 / >40	1.2 (Negative)
11	>40 / >40	>40 / >40	>40 / >40	1.1 (Negative)
12	>40 / >40	>40 / >40	>40 / >40	0.9 (Negative)
13	>40 / >40	>40 / >40	>40 / >40	0.2 (Negative)
14	>40 / >40	>40 / >40	>40 / >40	1.3 (Negative)

¹ Cycle threshold. ² Two gene targets, E and RdRp ³ current difference larger than 2 μ A was considered as positive sample

Conclusion

While PCR remains the gold standard method for the detection of SARS-CoV-2 infection, diagnostic methods that allow faster testing in a cost-effective manner and more easily implemented on a larger scale represent a step closer to mass screening with higher frequency. With POC or bedside analysis becoming a global trend in modern diagnostics, simplicity, sensitivity and selectivity are the main criteria for choosing an adequate system. Furthermore, reliable, reproducible sample collection becomes as important as diagnosis in POC testing devices. This intent of this work was to demonstrate the entire system from sampling to sensing and identification. The sensor selectively detects SARS-CoV-2 viral particles down to 10 pfu mL⁻¹ in cultured SARS-CoV-2 suspensions. Additionally, it is shown that converting exhaled breath vapor into EBC provides a convenient and accessible sample source for SARS-CoV-2 viral particles. Our work underlines that EBC can identify SARS-CoV-2 by RT-PCR in patients identified as SARS-CoV-2 positive on nasopharyngeal swab samples. Based on quantitative analysis of positive cases the virus in 5 min exhalations of patients into EBC collecting masks is detectable. It remains surprising that Sample 1 with a very low C_t value comes out as negative in EBC PCR and on the aptasensor. The sampling part is directly correlated viral load in breath and breathing of the patient. Some optimization therefore needs to be implemented to make the sampling step more robust to overcome some false negative issues. Eventual integration of the sensor into the mask itself would likely make the method even more robust and user-friendly (**Figure S1**). Nevertheless, the results validate the concept that the detection of SARS-CoV-2 in the breath of COVID-19 patients using a rapid aptasensor is feasible. This opens the path for a rapid personalized screening of the infectious state in a short time and potentially even in the home.

3. Experimental Part

Materials: 3-mercaptopropionic acid (98%), 1-ethyl-3-[3-dimethylaminopropyl]-carbodiimide hydrochloride (EDC), N-hydroxysuccinimide (NHS), ferrocenemethanol were purchased from Sigma Aldrich and used as-received. Phosphate saline solution (PBS 1 \times) was obtained from Thermo Fisher scientific. Maleimide-PEG₆-amine (MW 1kDa) was purchased from Interchim Uptima. Milli-Q water was used throughout the whole study. Recombinant

SARS-CoV-2 Spike Glycoprotein S1 was obtained from Amsbio, USA (Amsbio Cat.# AMS.SPN-C52H4). RBD UK was purchased at Sinobiological (Ref# 40592-V08H8), and RBD South African from Acrobiosystems (Ref# SPD-C52H).

The screen-printed electrodes used in this work were purchased from PalmSens (The Netherlands, distributed by Hdts in France) and are available under the name AUH3600-IPM-Intelligent Pollutant Monitoring Denmark. They consist of a 3 mm diameter gold working electrode, a silver/silver chloride reference, and a carbon counter electrode.

RTube condensers were purchased from Respiratory Research In, USA.

Mask-based EBC collectors: The mask-based EBC collector is currently fabricated in-house at Diagmetrics and consists of 30 cm wide rolls of 120 μm thick natural virgin Polytetrafluoroethylene (PTFE) sheet (eplastics.com., USA), 10 cm wide 3M 465 double sided adhesive transfer tape (uline.com, USA) were purchased as well as a super absorbent polymer (SAP) powder, MediSAP 715 (M2 Polymer Technologies, Inc. , Illinois, USA). A stamping jig was constructed from 0.315 cm PTFE plate (eplastics.com , USA) and the jig was cut on a 100W CO₂ laser cutter (Orion Motor Tech, China). A Digital Combo Heat Press (Geo Knight, Massachusetts, USA) was used to stamp the 127 μm thick PTFE sheet using the jig to form a pocket in the PTFE sheet for receiving a thermal mass mixture of water and the SAP. A second layer of the 127 μm PTFE sheet was bonded to the heat stamped 127 μm PTFE sheet using the 3M 465 adhesive, sandwiching the thermal mass of water/SAP between layers of PTFE sheet. The completed PTFE/thermal mass/3M 465/PTFE laminated sandwich was hand cut using scissors into the final shape of the EBC collector that is configured and dimensioned to be inserted into a pre-existing face mask or built into a newly constructed face mask. The EBC collector constructed as described was designed for and retro fit into various disposable face masks of different styles and construction, including N95 and KN95 made by 3M and overseas manufacturers. These masks are currently not commercially available, but were designed with eventual mass production in mind.

Immobilization of thiolated aptamer: All DNA aptamers (Base Pair Biotechnologies) were synthesized by standard phosphoramidite chemistry by IDT (Coralville, IA, USA). Gold electrodes were exposed to 10 μL of 3-mercaptopropionic acid (25 mM) in MQ-water for 30 min at room temperature. The surface was washed with MQ-water and dried in air. Then the acid-terminated surface was activated with EDC/NHS (1:1 molar ratio, 15 mM in PBS 1 \times , pH

7.4) for 20 min, followed by immersion into NH₂-PEG₆-maleimide (10 μL, 0.1 mg/mL in PBS 1×, pH 7.4) for 2 h at 4 °C and washing with MQ-water.

The aptamers were dissolved in 10 mM Tris, 0.1 mM EDTA (pH 7.5) at 100 μg mL⁻¹ and then mixed with 10 mM TCEP in a 1:1 ratio. The PEG₆-maleimide modified electrodes were incubated for 2 h with 10 μL of this solution and then washed copiously with MQ-water to remove excess aptamer and unreacted reagents. Finally, the electrodes were incubated 2 h with folding buffer then washed and dried. The surfaces were kept at 4°C until use.

Electrochemical measurements were performed with a Sensit-Smart smartphone potentiostat (Palmsens, The Netherlands, distributed by Hdts in France). Cyclic voltammograms were recorded at 50 mV s⁻¹ using ferrocenemethanol (1 mM, PBS 1×, pH 7=4) as redox mediator. The scan direction was from -0.1 V to 0.3 V and then back to -0.1.

Differential pulse voltammograms (DPV) were acquired in the appropriate potential range using the following DPV parameters: $t_{\text{acquis}}=3\text{s}$, $E_{\text{step}}=0.01\text{V}$, $E_{\text{pulse}}=0.06\text{ V}$, $t_{\text{pulse}}= 0.02\text{ V}$, scan rate=0.06 V s⁻¹. The diameter of the gold electrode was 3 mm ($A=0.071\text{ cm}^2$).

EBC collection and sensing: Before EBC collection, the engineered masks were placed for 20 min at -20°C (freezer), and then immediately worn for 5 min. During this 5 min, breathing with open mouth was performed, which resulted in the condensation of the breath on the Teflon-lining of the mask. After 5 min the mask was carefully removed, and the liquid droplets collected with a plastic pipette. Sensing was performed in two steps. First a DPV signal was recorded on the aptamer-sensor using ferrocenemethanol (1 mM, PBS 1×, pH 7=4) as redox mediator. Thereafter, the electrode was immersed into 5 mL of PBS 1× (pH 7=4) 2 times and 200 μL of the collected EBC deposited onto the working electrode. After 10 min incubation with the EBC samples, the electrode was immersed again into 5 mL of PBS 1× (pH 7=4) for 2 times and then into ferrocenemethanol (1 mM, PBS 1×, pH 7=4). A DPV was recorded using the same conditions as before. The difference in the maximal current before and after EBC contact was used for identification of the sample as positive or negative.

Virus isolates

Three SARS-CoV-2 patient isolates were used, one clade 20A.EU2, one clade 20I/501Y.V1 (GISAID: EPI_ISL_1653931) and one clade 20H/501Y.V2 (GISAID: EPI_ISL_1653932).

Virus Titration: Vero E6 cells (ATCC CRL-1586) were cultured in Dulbecco's modified Eagle medium (DMEM) supplemented with 10% fetal bovine serum (FBS), 1% L-glutamine, 1% antibiotics (100 U mL⁻¹ penicillin), in a humidified atmosphere of 5% CO₂ at 37 °C. Vero E6 cells were plated in 96-well plates (2.5 × 10⁵ cells/well) 24 h before performing the virus titration. Clinical isolates, obtained from SARS-CoV-2 positive specimens, was cultured on Vero E6 cells. Infected cell culture supernatant was centrifuged for 10 min at 1500 rpm at 4 °C to obtain a virus suspension. The virus suspension was used undiluted and in serial ten-fold dilutions. Virus suspensions were distributed in 6 wells in DMEM supplemented with 2% FBS (Fetal Bovine Serum) to Vero E6 cells, 1% antibiotics (100 U mL⁻¹ penicillin), and 1% L-glutamine. The plates were incubated for 6 days in 5% CO₂ atmosphere at 37 °C. The plates were examined daily using an inverted microscope (ZEISS Primovert) to evaluate the extent of the virus-induced cytopathic effect in cell culture. Calculation of estimated virus concentration was carried out by the Spearman and Karber method (Kärber, 1931, Spearman, 1908) and expressed as TCID₅₀/mL (50% tissue culture infectious dose). TCID₅₀/mL values were transformed to PFU/mL by using the formula PFU/mL= TCID₅₀/mL × 0.7.

SARS-CoV-2 RT-PCR: RNA was extracted from 140 µL of EBC using the QIAamp viral RNA mini kit (Qiagen) and eluted in 50 µL of buffer. RT-PCR for the E and RdRp genes was performed using the Eurobio Plex kit (Afzal, 2020). Undetectable SARS-CoV-2 levels were set to Ct>40. Amplification was performed on 7500 Real-Time PCR System (Applied Biosystems, USA).

Acknowledgements

Financial support from the Centre National de la Recherche Scientifique (CNRS), the University of Lille, I-SITE via the COVID task force and the Hauts-de-France region via ANR Resilience (CorDial-FLU) is acknowledged. The project is funded by the Horizon 2020 framework programme of the European Union under grant agreement no 101016038. The authors thank all personal at Cerballiance for their valuable help. The authors are thankful for all the volunteers who participated in this study, notably the inhabitants of Lille, Aniche and Villeneuve d'Ascq.

Declarations: Base Pair Biotechnologies authors GWJ and AC have a financial interest in the aptamers used in this study.

References

- Afzal, A. Molecular diagnostic technologies for COVID-19: Limitations and challenges, 2020. *J. Adv. Res.* 26, 149-159.
- Cannes, C., Kanoufi, F., and Bard, A. J. Cyclic voltammetry and scanning electrochemical microscopy of ferrocenemethanol at monolayer and bilayer-modified gold electrodes, 2003. *J. Electroanal. Chem.* 547, 83-91.
- Da Pieve, C., Williams, P., Haddleton, D. M., Palmer, R. M. J., and Missailidis, S. Modification of thiol functionalized aptamers by conjugation of synthetic polymers, 2010. *Bioconjug. Chem.* 21, 169-174.
- Eiche, T., and Kuster, M. Aerosol release by healthy people during speaking: possible contribution to the transmission of SARS-CoV-2., 2020. *Ijerp*. 17, 9088.
- Giovannini, G., Haick, H., and Garoli, D. Detecting COVID-19 from Breath: A Game Changer for a Big Challenge, 2021. *ACS Sens.* 6, 1408-1417.
- Kärber, G. Beitrag zur kollektiven Behandlung pharmakologischer Reihenversuche, 1931. *Arch F Exp Pathol U Pharmakol* 162, 480–483.
- Khoubnasabjafari, M., Jouyban-Gharamaleki, V., Ghanbari, R., and Jouyban, A. Exhaled breath condensate as a potential specimen for diagnosing COVID-19, 2020. *Bioanalysis* 12, 1195-1197.
- Leung, N. H. L., Daniel K. W. Chu, E. Y. C. S., Kwok-Hung Chan, James J. McDevitt, Benien J. P. Hau, Hui-Ling Yen, Yuguo Li, Dennis K. M. Ip, J. S. Malik Peiris, Wing-Hong Seto, Gabriel M. Leung, Donald K. Milton & Benjamin J. Cowling , and Nature Medicine volume 26, p. C. t. a. Respiratory virus shedding in exhaled breath and efficacy of face masks, 2020. *Ned. Med.*
- Manochery, S., McConnell , E. M., and Li, Y. Unraveling Determinants of Affinity Enhancement in Dimeric Aptamers for a Dimeric Protein, 2019. *Sci. Rep.* 9, 17824
- Ryan, D. J., Toomey, S., Madden, S. F., Casey, M., Breathnach, O. S., Morris, P. G., Grogan, L., Branagan, P., Costello, R. W., De Barra, E., et al. Use of exhaled breath condensate (EBC) in the diagnosis of SARS-COV-2 (COVID-19), 2021. *Thorax* 76, 86-88.
- Saroglia, L. F., and Galatà G, D. S. R., Fillo S, Luca V, Faggioni G, D'Amore N, Regalbuto E, Salvatori P, Terova G, Moscone D, Lista F, Arduini A. A reliable and miniaturized electrochemical immunosensor for SARS-CoV-2 detection in saliva 2021. *Biosens. Bioelectron* 171, 11286.
- Seo, G., Lee, G., Kim, M. J., Baek, S.-H., Choi, M., Ku, K. B., Lee, C.-S., Jun, S., Park, D., Kim, H. G., et al. Rapid Detection of COVID-19 Causative Virus (SARS-CoV-2) in Human Nasopharyngeal Swab Specimens Using Field-Effect Transistor-Based Biosensor, 2020. *ACS Nano* 14, 5135-5142.
- Shan, B., Broza, Y. Y., Li, W., Wang, Y., Wu, S., Liu, Z., Wang, J., Gui, S., Wang, L., Zhang, Z., et al. Multiplexed Nanomaterial-Based Sensor Array for Detection of COVID-19 in Exhaled Breath, 2020. *ACS Nano* 14, 12125-12132.
- Song, Y. S., J. , Wei, X., Huang, M., Sun, M., Zhu, L., Lin, B., Shen, H., Zhu, Z., and Yang, C. Discovery of Aptamers Targeting Receptor-Binding Domain of the SARS-CoV-2 Spike Glycoprotein, 2020. *Anal. Chem.* 92, 9895-9990.
- Spearman, C. T. The Method of “Right and Wrong Cases” (Constant Stimuli) without Gauss’s Formula., 1908. *Br. J. Psychol.* 2, 227–242.
- Szunerits, S., Pagneux, Q., Swaidan, A., Mishyn, V., Roussel, A., Cambillau, C., Devos, D., Engelmann, I., Alidjinou, E. K., Happy, H., et al. The role of the surface ligand on the performance of electrochemical SARS-CoV-2 antigen biosensors, 2021. *Anal. Bioanal. Chem.* accepted.

- Ter-Ovanesyan, D., Gilboa, T., Lazarovits, R., Rosenthal, A., Yu, X., Z. Li, J. Z., Church, G. M., and Walt, D. R. Ultrasensitive Measurement of Both SARS-CoV-2 RNA and Antibodies from Saliva., 2021. *Anal. Chem.* 93, 5365-5370.
- Torabi, R., Ranjbar, R., Halaji, M., and Heiat, M. Aptamers, the bivalent agents as probes and therapies for coronavirus infections: A systematic review, 2020. *Molecular and Cellular Probes* 53, 101636.
- Vinkenburg, J. L., Mayer, G., and Famulok, M. Atamer-Based Affinity Labeling of Proteins*, 2012. *Angew. Chem. Int. Ed.* 51, 9176 –9180.
- Wrapp, D., and Wang N, C. K., Goldsmith JA, Hsieh C-L, Abiona O, et al. . Cryo-EM structure of the 2019-nCoV spike in the prefusion conformation., 2020. *Science* 367, 1260–1263.
- Wyllie, A. L., Fournier, J., Casanovas-Massana, A., Campbell, M., Tokuyama, M., Vijayakumar, P., Warren, J. L., Bertie Geng, B., Muenker, M. C., Moore, A. J., et al. Saliva or Nasopharyngeal Swab Specimens for Detection of SARS-CoV-2., 2020. *N. Engl J Med.* 383, 1283-1286.
- Yoo, H., Jo, H., and Oh, S. S. Detection and beyond: challenges and advances in aptamer-based biosensors, 2020. *Mater. Adv.* 1, 2663-2687.
- Zhang, L., Fang, X., Liu, X., Ou, H., Zhang, H., Wang, J., Li, Q., Cheng, H., Zhang, W., and Luo, Z. Discovery of sandwich type COVID-19 nucleocapsid protein DNA aptamers, 2020. *Chem. Commun.* 56, 10235.